CHAPTER - III

ELECTRICAL PROPERTIES

SECTION - A

D.C. Electrical Resistivity

3. Introduction

Historically, ferrites have attracted the attention of many physicists and technologists as they are the important semiconductor materials. Both the semiconductor and magnetic material exhibit interesting properties that could be used in electronic devices. The mechanism of charge transport plays a very important role in development of electrical properties. The information of interest for an empirical analysis of conduction process is the density and mobility of charge carriers as a function of temperature and types of energy levels which the carriers occupy. The electrical conductivity of ferrites mainly depends upon the chemical composition, temperature, porosity, density and method of preparation.

The room temperature resistivity of pure NiO, Fe_2O_3 and of some ferrites and garnets exceeds 10^{10} Ω cm. that they can be regarded practically as insulators. For oxides which contain a substantial concentration of metal ions, in two different valence states on crystallographically equivalent sites, require relatively small activation energies [1] and this is reflected in low resistivities. The conductivity for a given oxide system increases with mixed valency concentration [2,3].

The spin alignment and electrical conduction relationship can be inferred from comparison of conductivity versus temperature studies observed below Curie or Neel temperature. With high temperature paramagnetic region, for many oxides, the spontaneous magnetization does not affect the electrical transport properties. Certain oxides exhibit a marked change in the slope of Log ρ versus $1/T \times 10^3$ relationship, whereas magnetie (Fe_3O_4) undergoes a semiconductor to metal transition [4].

The conduction in ferrites is mainly due to exchange of 3d electrons, localized at metal ions i.e. from Fe^{2+} to Fe^{3+} and vice versa [5]. Jonkar [6] derived an expression for mobility from hopping conduction model, based on the localized levels for electrons. Band polaron model based on electron transition between localized cell was also suggested [7]. Small polaron model has been introduced by Naubenreisser [8]. Lorentz and Ihle [9] have explained the electrical properties on the basis of thermally activated motion of electrons and Shrinivasan [10] has adopted phonon induced tunneling.

The electrical properties of ferrites are affected by the distribution of cations in the sites, magnetic and non-magnetic substitutions, the amount of Fe^{2+} present, sintering condition, grain size and grain growth effects etc. The electrical properties of Nickel ferrites have been studies by several investigators [11-14]. Van Uitert [13] investigated the effect of iron stoichimetry and sintering temperature on the resistivity of Nickel ferrites. Murthy and Sobanadri [15] have investigated the d.c. conductivity of some Ni-Zn ferrites as a function of temperature from room temperature to 300 °C. The ferrites which contains iron in excess shows n-type conduction and those with iron deficiency, show p-type conduction. The d.c. resistivity in Ni-Cd ferrites is investigated by Patil M.G. et. al. [16]. The effect of Al^{3+} substitution on electrical properties of Ni-Sn ferrites is investigated by Babbar and Chandel [17]. Ni-Sn ferrites of different compositions have been investigated by various other workers [18,19,20].

Section A

3.A.1 Conduction in Oxides

In oxides, oxygen ion are nearly on closed packed lattice, while cations are partly in octahedral sites and partly in tetrahedral sites. Such a oxide has spinel type crystal structure e.g. magnetite (Fe_3O_4). The structure of it can be described by

$$[Fe^{3+}]_A\ [Fe^{2+}\ Fe^{3+}]_A\ O_4^{2-}$$

This denotes that 1/3 of iron ions (all having +3 valances) are on tetrahedral site and remaining two thirds are on octahedral sites. In oxides the activation of conduction electron can be represented by,

$$O^{2-}-M^{2+}-O^{2-}-M^{2+}-O^{2-} \text{ ---- } O^{2-}-M^{1+}-O^{2-}-M^{3+}-O^{2-}$$

where, M is the divalent transition metal ion. The energy needed for the formation of ions pairs (M^{2+} M^{2+}) and (M^{3+} M^{1+}) corresponds to the gap in density of states.

3.A.2 Conduction in ferrites

At room temperature ferrites have wide range of resistivities from 10^{-3} to 10^{11} Ω cm. The low and high resistivities of ferrites are mainly explained on the basis of actual location of cations in spinel structure and hopping mechanism. Their high conductivity is due to simultaneous presence of ferrous and ferric ions in crystallographically equivalent sites. The high resistivity in ferrite is associated with the occupation of B-sites by divalent metal ions and trivalent iron ion. Such a arrangement requires higher activation energy for hopping of electrons. The two mechanism of conductivity can be represented as,

$$Fe^{2+} + Fe^{3+} \longleftrightarrow Fe^{3+} + Fe^{2+} + \Delta E$$

$$Me^{2+} + Fe^{3+} \longleftrightarrow Me^{3+} + Fe^{2+} + \Delta E \quad \ldots (3.1)$$

where ΔE is activation energy. The energy required to transfer of electron from Me^{2+} to Fe^{3+} and vice versa. Me denotes divalent metal ion like Cu, Co, Mg, Mn, Ni and Cd etc.

The free electron model cannot explain the electrical conductivity of ferrites because of the fact that the electrons in ferrites are not free and energy band model is not suitable to explain the electrical conductivity for the lack of Bloch type wave functions for the electrons in ferrites. The conductivity of ferrite can be however explained in terms of electronic charge carriers like electrons and holes by the relation,

$$\sigma = e\,(ne\mu e + nh\mu h) \qquad \ldots \qquad (3.2)$$

where n and μ stand for concentration and mobilities of electrons(e) and holes (h) respectively. As electron moves in one direction, the holes move in opposite direction. Though the velocities of electrons and holes are the same, mobility of electron is much higher than mobility of holes.

The hopping mechanism of conductivity in ferrite is associated with activation energy which can be calculated from log ρ vs 1/T plots. As temperature increases, the ferrite changes its magnetic state from a ordered ferrimagnetic state to a disordered paramagnetic state. When such a change occurs there is an abrupt change in activation energy. It is observed that, activation energy in ferrimagnetic region is less than the activation energy in paramagnetic region.

In ferrite, two types of scatterings exist, the phonon scattering arising out of thermal vibration of lattice and the impurity scattering. The lattice scattering increases with increasing amplitude of vibration at higher temperature. The mobility is proportional to the mean free path between scattering event. Hence conductivity becomes temperature dependent and it is written as,

$$\sigma = \sigma o \ \exp. \ (-\Delta E \ /KT) \qquad \ldots \qquad (3.3)$$

where, σo – temperature dependent constant

K – Boltzman constant

Further, in ferrite lattice, there is an interaction between orbitals of neighbouring ions and electrons resulting into the polarization of lattice. This effect is more pronounced due to strong coulomb interaction in ionic crystals such as ferrites. The combination of an electron and its polarization field is called as 'polaron'.

When such an association is weak it constitutes large polarons. Such polarons are found in ionic crystals and conductivity of ionic crystal is similar to the one explained above. But when electron plus lattice deformation has a linear dimension smaller than lattice constant, it constitutes small polarons. They are usually found in covalent crystals. Due to such a deformation the effective mass of electron increases as it partically drags the ions along with it. Therefore, mobility of electron decreases and becomes highly temperature dependent. With the help of binding energy

Ep of electron and polarized lattice, the mobility of electron be written as,

$$\mu_{polaron} \; \alpha \; \exp. \; (-E_p/KT) \qquad \ldots \quad (3.4)$$

where $E_p = e^2/K_{eff}.V_p$

where, Vp = dimension of lattice deformation

$1/K_{eff}$ = difference of reciprocal of optical and static dielectric constant

The mobility is always less then 1 cm^2/v-sec and is very low. With the help of small polarons the conductivity is related to Eg, Ep and T by relation

$$\sigma = n\mu \; \exp \; (-Eg/KT).(-Ep/KT) \qquad \ldots \quad (3.5)$$

Due to polarization, the electrons are trapped at the potential well. When such a potential well is deep enough, the electron may be trapped at lattice site. Therefore, its transition to neighbouring site may be governed by thermal activation. Hence due to thermal activation lattice is set into periodic vibrations which are quantized into phonons.

At high temperatures electrons jump from one site to another by thermal activation. The hopping mechanism contributes to conductivity at high temperature. At low temperature electrons tunnel slowly through crystal resulting into small conductivity.

The temperature dependence of mobility (μ) is given by [21]

$$\mu = \frac{e^2a^2w^2}{KT} \exp \left(\frac{-E}{KT}\right) \qquad \ldots \quad (3.6)$$

where, w - polaron frequency

a - distance between the neighbouring site i.e. jump length

At low temperatures, polarons behave as particles moving in the narrow band, where as at high temperatures small polaron motion results by the absorption of one or more phonons. Therefore, the process is essentially a hopping mechanism. When a tunneling time is less than the time for successive hopping transition, conduction by small polaron becomes more predominant. The small polaron model for conductivity mechanism is explained earlier [22-26].

From the plot of logarithm of resistivity versus reciprocal of temperature, it is noticed that the slope of log ρ Vs $1/T \times 10^3$ K^{-1} curve changes at a particular temperature which is identified as Curie temperature (Tc). It is also observed that resistivity of samples decreases with increasing temperature. The variation of resistivity with temperature obeys the exponential relation,

$$\rho = \rho_o \exp(-\Delta E/KT) \qquad \dots \quad (3.7)$$

where, ΔE - activation energy and can be interpreted as the energy required to cause the electron jump.

The change in slopes is due to disordering of electron spin at that temperature (Tc). These breaks suggest that, there is some predominant change in conduction mechanism due to magnetic phase transition.

The high activation energy is associated with a high resistivity at room temperature. The dependence of resistivity on the stoichiometry was studied by Van Uitert [13] and Jonkar [27].

In stoichimetric Ni ferrites there is some tendency for valency changes according to,

$$Ni^{2+} + Fe^{3+} \rightleftharpoons Ni^{3+} + Fe^{2+}$$

both the Nickel and iron ions, having two different valencies, provided conductivity mechanism. On the other hand, the presence of Al makes the valency changes,

$$Ni^{3+} + Al^{2+} \rightleftharpoons Ni^{2+} + Al^{3+}$$

$$Fe^{2+} + Al^{3+} \rightleftharpoons Fe^{3+} + Al^{2+}$$

Both the divalent iron and trivalent nickel will be suppressed. When Al ions are present in two valence states, these will be widely separated and thus division of electrons through the lattice will require considerable activation energy.

3.A.3 Experimental Techniques

The experimental set up for d.c. electrical resistivity is shown in Fig. 3.A.1. It consists of an electrically heated furnace, a digital d.c. microvoltmeter and a transistorized power supply unit (TPSU) to provide the d.c. voltage. The silver paste was applied on both sides of the pellet for good ohmic contacts. The pellet was mounted in a sample holder

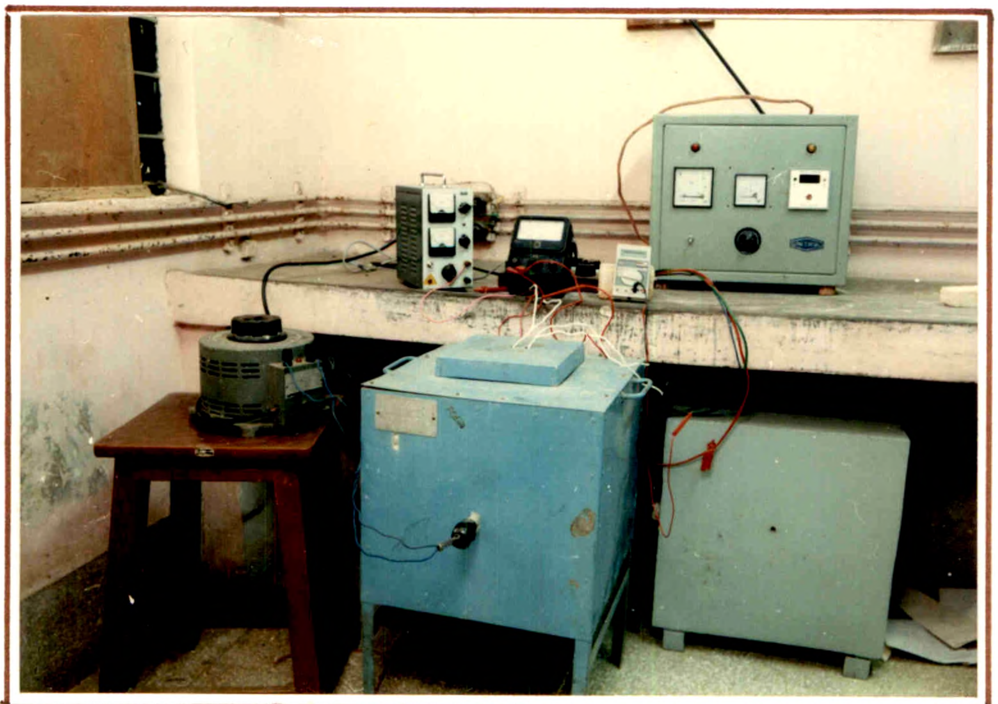

FIG.3.A.1. EXPERIMENTAL SET UP FOR D.C. ELECTRICAL RESISTIVITY MEASUREMENT.

consisting of two steel rods, in which the sample can be sandwiched tightly with the help of screws. The cell was then placed in a furnace. A calibrated Cromel-Alumel thermocouple was used to measure the temperature of furnace. Resistivity measurement were carried out by measuring the current at a constant voltage of 5 volts from room temperature to 925 °K and resistivity [9] was determined by the relation

$$\rho = \pi r^2/t \cdot V/I$$

where, t – thickness of pellet

r – radius of pellet

i – current through the sample

3.A.4 Results and Discussion

The present results on the measurement of d.c. resistivity of $NiAl_xFe_{2-x}O_4$ series are plotted in Fig. 3.A.2 for x = 0.2, 0.4, 0.6, 0.8 and 1.0 respectively. It is observed that slope of log ρ versus $1/T \times 10^3$ K^{-1} changes at a particular temperature which is identified as Curie temperature. It is also observed that resistivity of the samples in general increases with Al content and decreases with increasing temperature.

The observed discontinuities in the log ρ versus $1/T \times 10^3$ K^{-1} have been attributed to several reasons by different authors. It has been stated by Irkhin et. al. [30] that change in the slope of the straight line should occur while passing through the Curie point. The

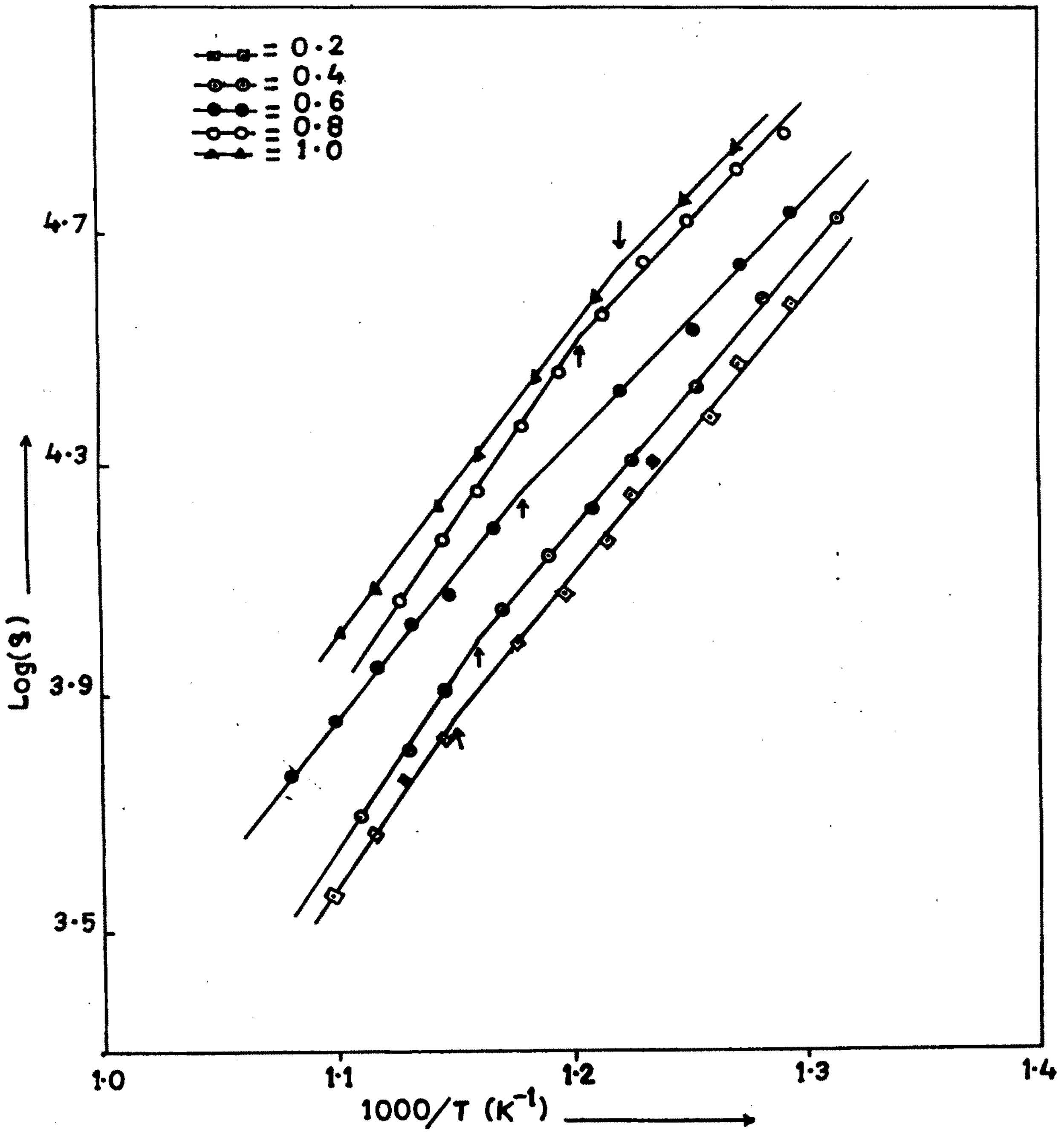

Fig.3.A.2. Variation of Log(ρ) Vs.(1000/T) for $NiAl_xFe_{2-x}O_4$ series.

point separates the upper ferrimagnetic region from lower paramagnetic region, as the spin-spin interaction vanishes due to thermal vibrations. Similar result have been reported by Komar and Klivshin [29] in the case of several other ferrites and they have stated that the change in the activation energy of conduction at a particular temperature has some relation with the ferrimagnetic Curie temperature of the ferrites. Such a proof for a evidence of a relation between magnetic ordering and conductivity also comes from the present results. The breaks in the conductivity plots may also be due to some other reasons like conduction mechanism [31]. The effect of Al^{3+} substitution in Ni-Zn ferrite shows such discontinuities as studied by Chandra Prakash [32]. Similar results are reported by Kakatkar [33].

The magnetic order in spinel ferrites is mainly due to superexchange interaction mechanism occuring between metal ions in A and B sublattices (34).

There are three types of interactions in ferrites namely A-A, A-B and B-B interactions. Nonmagnetic Al ions occupy positions in B-sublattice and this causes decrease in both A-B and B-B interaction. So the B-B interaction which is responsible for conduction decreases with increasing aluminium content.

During sintering some Fe^{3+} change to Fe^{2+} so the electronic conductivity occurs due to exchange of electrons between trivalent iron ion and divalent iron ion on octahedral sites. The existence of B-B exchange interaction between ions on the B-sites of such a ferrite will affect the activation energy required for transfer of electrons between Fe^{2+} and Fe^{3+}.

The activation energies corresponding to the para and ferrimagnetic regions (high and low temperature regions respectively Fig. 3.A.2) were calculated using equation (3.7) and are presented in Table (3.A.1). The activation energy in paramagnetic region is found to be higher than that of ferrimagnetic region in agreement with the theory developed by Irkhin and Turov [34]. Similar results were also observed for many ferrites [35,36,6].

The transition temperature Tc from log ρ versus $1/T \times 10^{3}\ K^{-1}$ plots are given in Table 3.A.1. From this Table it can be seen that transition temperature (Tc) decreases with increasing Al content [Fig. (3.A.3)]. Such a variation can be explained on the basis of the strength of exchange interaction between the magnetic ions, which in turn depends upon their density and magnetic nature. As the number of Al^{3+} ions increases in the samples, the number of Fe^{3+} ions go on decreasing. This decreases the A-B interaction. The thermal energy required to offset the magnetic order decreases and hence Tc decreases.

TABLE - 3.A.1.

Activation energy and Curie Temperature data for

$NiAl_xFe_{2-x}O_4$

X	Activation Energy 'ΔE' (ev)		Curie Temp.
	ΔE_{ferri} ev	ΔE_{para} ev	T_c °C
0.2	0.954	1.156	571
0.4	0.917	1.192	556
0.6	0.795	1.0212	549
0.8	0.874	1.156	525
1.00	0.848	1.0595	515

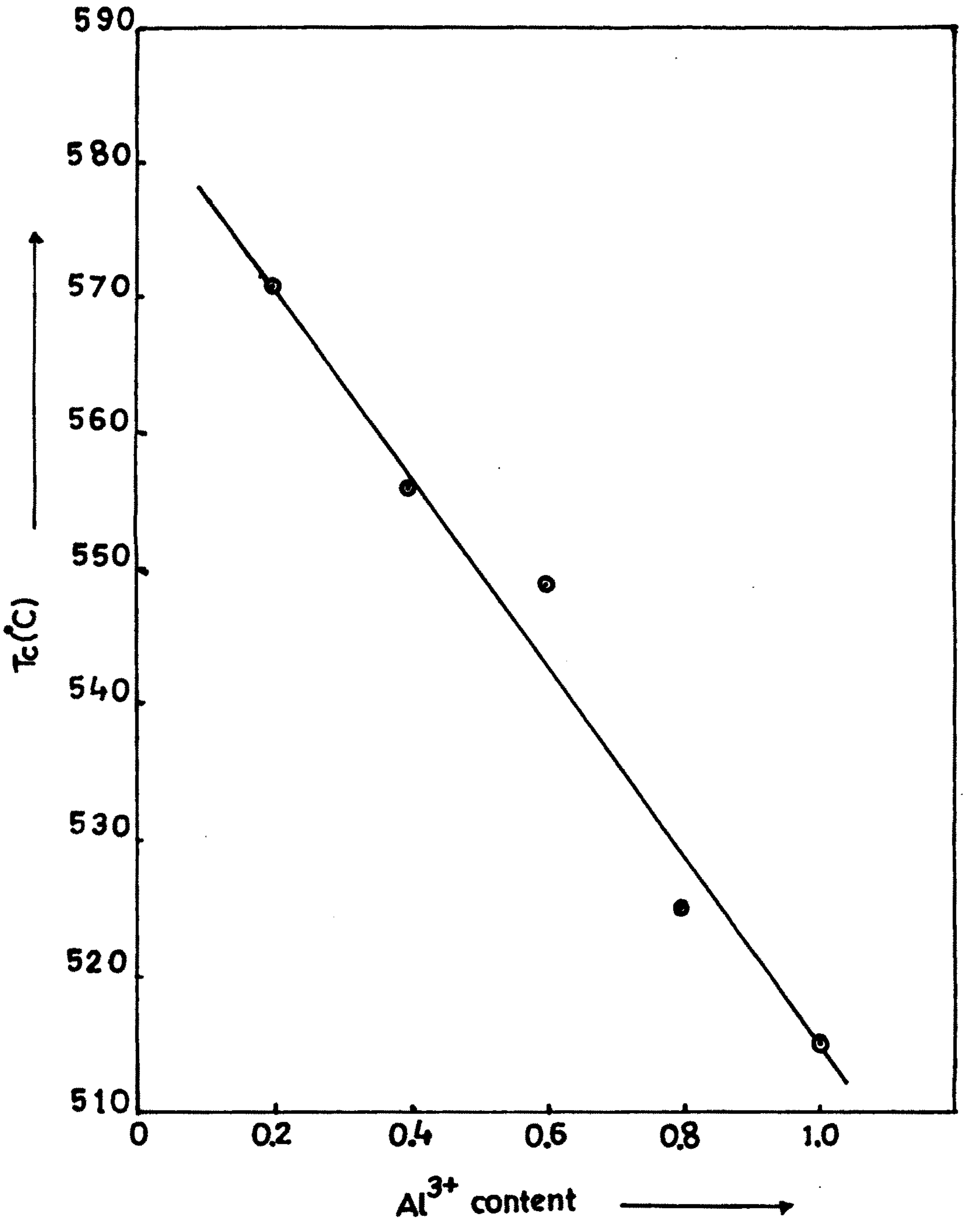

Fig. 3.A.3. Variation of Curie Temp. With Al^{3+} Content

SECTION - B

THERMOELECTRIC POWER

3.B.1. Introduction

In ferrites, thermoelectric power and Hall effect properties are used in the interpretation of the conduction mechanism. The interpretation of Hall effect is more straight forward and it gives precise results. However, in case of low mobility materials such as ferrites, it is sometimes difficult to measure the Hall effect. In such cases, the thermoelectric power is the only alternative. However, the measurement of the thermoemf is simple and its sign gives vital information about the type of conduction whether they are n-type or p-type [37]. Another importance significance of thermoemf is that it enables one to calculate the values of Fermi energy and carrier concentration [38].

Seebeck effect is due to diffusion of electrons or holes which have more kinetic energy at hotter surface and hence the emf is produced. According to quantum theory for semiconductors, 'α' for both type of carriers is given by,

$$\alpha = \frac{\alpha_n\sigma_n + \alpha_p\sigma_p}{\sigma_n + \sigma_p}$$

where, $\sigma_n = n_e\mu_n$

$\sigma_p = p_e\mu_p$

$\alpha_n = (k/e)\ (A_n - E_f/KT)$

$$\alpha_p = (K/e)\ [A_p + (E_g+E_f/KT)]$$

where n and p are electron and hole densities, μn and μp are electron and hole mobilities. Ef is Fermi energy and Eg is band gap energy.

The temperature dependence of thermoelectric power for ferrite materials having only one type of charge carriers can be expressed as [39]

$$\alpha = \left(\frac{K}{e}\right) \left[\log\left(\frac{No}{n} - 1\right) + \frac{e}{KT}\right] a$$

where K - Boltzman constant

e - electronic charge

No - concentration of trivalent ions on octahedral sites

n - concentration of Fe^{2+} ions

a - is part of activation energy transported by the electrons

T - absolute temperature

From temperature dependence of Seebeck coefficient, the sign of charge carriers have been determined.

3.B.2 Experimental Techniques

The experimental set up for thermoelectric power measurement is shown in Fig. 3.B.1. It consist of a furnace, d.c. microvoltmeter, sample holder and digital multimeter.

the surface of pellets were coated with silver paste for good ohmic contacts. The pellet was put in

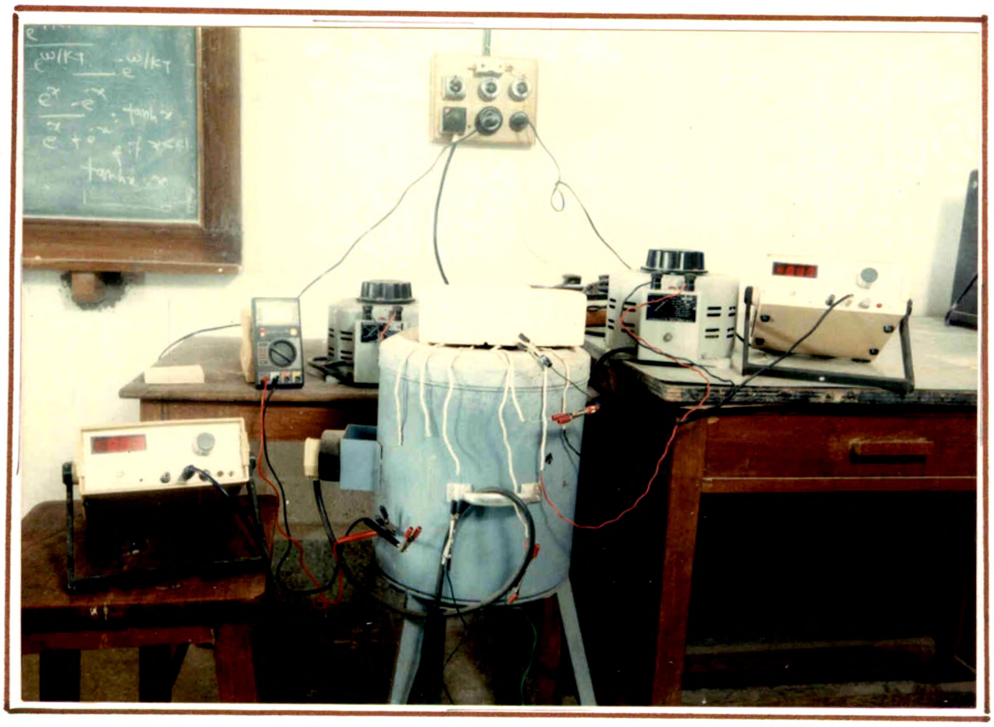

FIG.3.B.1. EXPERIMENTAL SET UP FOR THERMO-EMF MEASUREMENT

the sample holder and then kept into furnace for the measurement of thermoelectric power. The temperature difference of 20 °C across the pellet was measured on a digital d.c. microvoltmeter. The sample was then heated in furnace and thermoemf was measured at different temperatures. In the measurement of thermoemf, microvoltmeter gives positive deflection by connecting its positive terminal to hot end of the sample. This happen in case of n-type charge carriers. This situation reverses when charge carriers are of p-type.

The thermoelectric power was determined by using the relation

$$\alpha = \frac{\Delta V}{\Delta T}$$

where ΔV - thermoemf

ΔT - temperature difference across the pellet

The sign of thermoemf is determined from the polarity of the cold end of the specimen as the charge carriers diffuse from hot to cold part.

3.B.3 Results and Discussion

The variation of Seebeck coefficient (α) as a function of temperature for the system $NiAl_xFe_{2-x}O_4$ with x = 0.2, 0.4, 0.6, 0.8 and 1.0 is shown in Fig. 3.B.2.

From the plots it can be seen that, for the sample with x = 0.2 thermoelectric power is negative

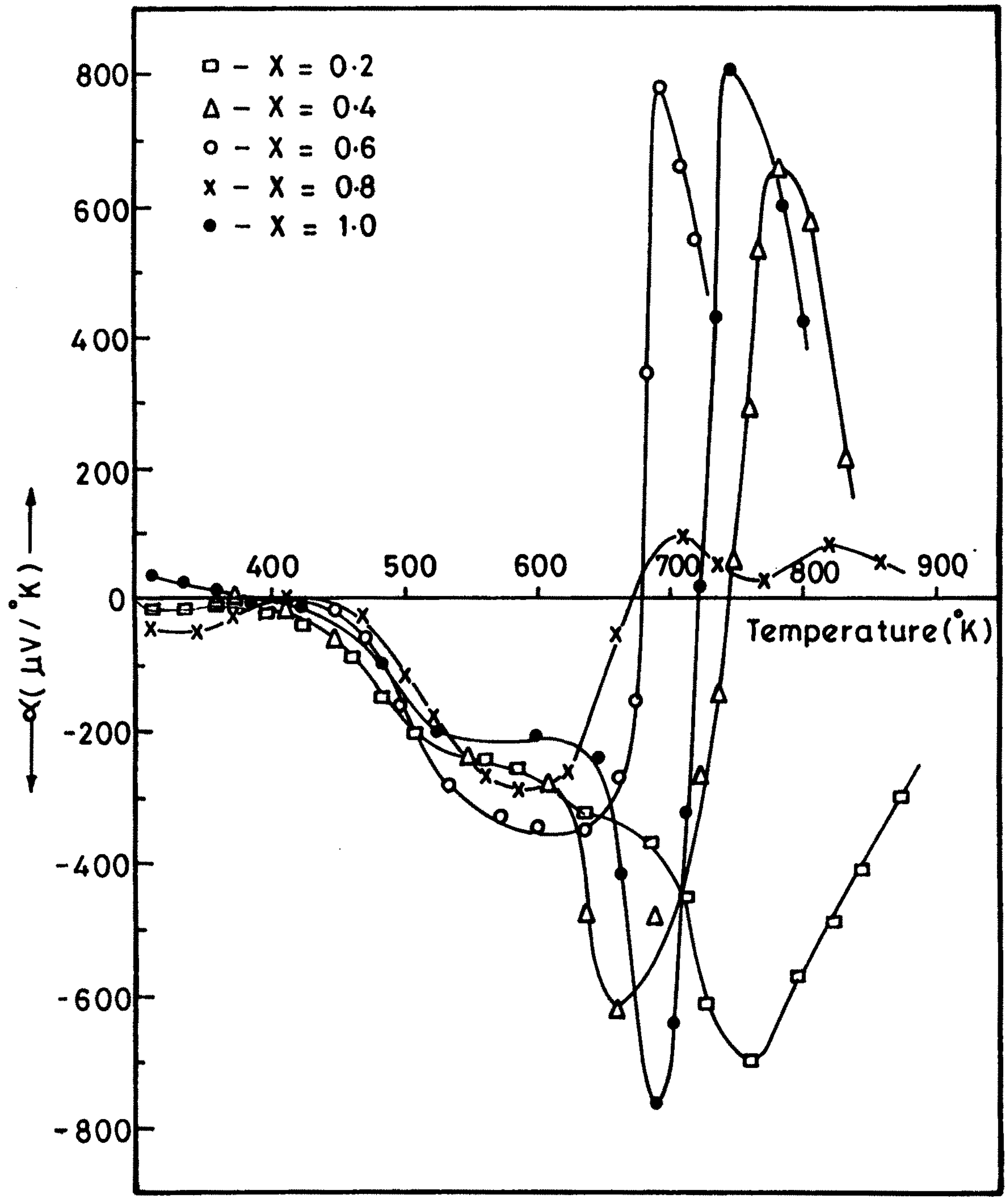

FIG.3.B.2. TEMPERATURE VARIATION OF THERMOELECTRIC POWER FOR $NiAl_xFe_{2-x}O_4$ SERIES.

indicating that, electrons are majority carriers. It increases in magnitude with temperature, which might be due to activated electron between Fe^{2+} and Fe^{3+} in octahedral sites. For x = 0.4, 0.6 and 0.8 initially thermoelectric power is negative then it changes to positive sign as the temperature increases. Thus it shows that both type of charge carriers are present in these samples.

For x = 1, at room temperature thermoelectric power is positive indicating that holes are majority carriers. It decreases with temperature changes to negative sign at about 385 °K and increases in the same direction because the activation energy for electron hopping is less than that for holes.

The presence of nickel on octahedral sites favours the conduction mechanism [40] a,

$$Ni^{2+} + Fe^{3+} \rightleftharpoons Ni^{3+} + Fe^{2+}$$

thus the conduction mechanism for n-type is predominantly due to hopping of electrons [41] from

$$Fe^{2+} + e^{-} \Longrightarrow Fe^{2+}$$

Whereas the conduction mechanism in p-type samples is predominantly due to hole transfer from Ni^{3+} to Ni^{2+} ions,

$$Ni^{2+} + h \Longrightarrow Ni^{3+}$$

References

1. Varnom M.W. and Lovell M.C.
J. Phys. Chem., Chemi., Soc., 27 (1966) 1125

2. Miyata N.
J. Phys. Soc. Japan 16 (1966) 206

3. Jonkar J.H. and Van Santen S.
Physica 19 (1953) 120

4. Craik D.J.
Magnetic Oxides,
Wiley Science (1975)

5. Bossman A.J. and Creve C.C.
Phys. Rev. 144 (1963) 763

6. Jonkar G.H.
J. Phys. Chem. Solids 9 (1959) 165

7. Dogoue R.R., Cerenkov A.A. and Chimadzbove Yu.
Sovt. Phys. Solid State 3C (1961) 2698

8. Haubenreisser W.
Phys. Stat. Solidi 21 (1961) 3905

9. Lorentz B. and Ihle D.
Phys. Stat. Solidi 63 (1974) and 69 (1975) 451

10. Shrinivasan G.
Phy. Stat. Solidi 57 (1980) k1 79

11. Guillaud C. and Bertrand R.
J. Des. Res. `Conf. Mat. Res. Scientific' 3 (1950) 73

12. Van Uitert L.G.
Proc. I.R.E. 44, (1956) 1294

13. Van Uitert L.G.
J. Chem. Phys. a) 24 (1956) 306
b) 23 (1956) 1883

14. Subrahmanyam K.N. and Sweden S.A.
Phys. Stat.Solidi (a) 61 (1980) 59

15. Murthy V.R.K. and Sobhandri J.
Phys. Stat. Solidi (a) 38 (1976) 647

16. Patil M.G. et. al.
Bull. Mater. Sci., Vol. 17, 4 (1994), 399-403

17. Babbar V.K. and Chandel J.S.
Bull. Mater. Sci., Vol. 18, 8 (1995) 997

18. Varshney V., Puri R.K., Rao K.H. and
Mediratta R.G.
Proc. 3rd Conf. Ferrites (Japan) (1980) 207

19. Chandal J.S., Sud S.P. and Baijal J.S.
Proc. Solid State Phys. Symp. (India) (1988) 239

20. Baijal J.S., Kothari D. and Phanjoubam S.
Advances in Ferrites (edi.) Srivastava and
Patni M.J.
Oxford and IBH Pub. Co. New Delhi, 1 (371)

21. Heiks R.R. and Johnson W.D.
J. Chem. Phys. 26 (1957) 582

22. Yamashita J. and Kurasawa T.
J. Phys. Chem. Solids 5 (1958) 34

23. Holstein T.
Ann. Phys. (NY) 8 (1959) 343

24. Austin L.G. and Mott N.F.
Adv. Phys. (1969) 18

25. Apel J.
Sol. Stat. Phys. 18 (1969) 41

26. Gillot B.
Mat. Res. Bull. 11 (1976) 848

27. Jonkar G.H.
Phys. Grav. 22 (1956) 707

28. Bradley F.N.
Materials for Magnetic Function
Hayden Book Co., (New York) 78

29. Komer A.P. and Klivshin V.V.
Izv. Akad. Nauk. SSSR, Ser. Fiz. 18 (1954) 56

30. Irkhin P. and Turov E.A.
Fiz. Met. Metallved 4 91957) 582

31. Sawant S.R. and Patil R.N.
Solid State Commn. 40 (1981) 391

32. Chandra Prakash
J. Mater. Sci. Letters 6 (1987) 651

33. Kakatkar S.V.
Ph.D. Thesis, Shivaji University, Kolhapur (1994)

34. Irkhin Yu. P. and Turov E.A.
Sov. Phys. JETP 133 (1957) 673

35. Suryavanshi S.S.
Ph.D. Thesis, Shivaji University, Kolhapur (1990)

36. Otari S. M., Kadam V. B., Sawant S. R., and Patil S. A.
Ind. J. pure and applied physics. 28 (1990) 248.

37. Reddy P. V. and Rao T. S.
Phys. Stat. Sol. (a) 92, (1985) 303-307

38. Vishwanathan B., Murthy V. R. K.
`Ferrite materials'. Narosa publishing house
New Delhi (1990) 38.

39. Rosenberg M., Nicolan P. and Bunzet C.
Phys. Stat. Solidi, 15 (1966) 521

40. J. Smit and H. P. Wijn
"ferrites", Cleaver-Hume Press Ltd. London
(1959) 232

41. Van Uitert L.G.,
"J. Chem. Phys. 23, (1955) 1883.